3-Dimensional Classification and Visualization of Clouds simulated by Cloud-Resolving Atmospheric General Circulation Model

Daisuke Matsuoka[1] and Kazuyoshi Oouchi[1]

[1] Japan Agency for Marine-Earth Science and Technology (JAMSTEC), Yokohama, Japan
{daisuke, k-ouchi}@jamstec.go.jp

Abstract. Cloud-resolving atmospheric general circulation models using large scale supercomputers reproduce realistic behavior of atmospheric field on a global scale. To understand the simulation result for scientists, visualizing individual clouds and their physical characteristics is necessary. In this study, we propose a new feature extraction and classification method of simulated clouds based on their 3-dimensional shape and physical properties. The results of applying the proposed method show the clouds' distribution of a tropical cyclone during its generation, development and disappearance process, and the relation between cloud-forms and precipitation.

Keywords: Visualization, atmospheric simulation, cloud, feature extraction, classification

1 Introduction

Atmospheric phenomena such as a weather front, heavy rain and tropical cyclone affect the lives of human beings. Understanding these phenomena is important for social issues as well as academic issues. A large number of studies have been conducted in atmospheric and climate science fields by numerical simulations [1]. The conventional global atmospheric models based on primitive equations with hydrostatic approximation are not able to resolve individual clouds. Recently, because of the advances in supercomputing technology, NICAM (Non-hydrostatic Icosahedral Atmospheric Model) [2, 3] was developed for the Earth Simulator. NICAM calculates vertical flow without hydrostatic approximation and is able to reproduce vertical convection and *O*(10km) to *O*(100km) cloud clusters and is used to analyze MJO (Madden-Julian Oscillation)[4], tropical cyclones [5] and other global phenomena.

Generally, clouds have various types strongly related to atmospheric phenomena. To deeply understand such phenomena, understanding individual clouds and their physical properties is necessary. The latest cloud-resolving model can calculate the 3-dimensional (3D) configuration of individual clouds accurately; however, most previous studies for automatic cloud classification are intended at 2-dimensional (2D) simulation using satellite observational data (i.e. [6, 7, 8, 9]) and ground based imagery data (i.e.

[10, 11]) based on the color of clouds. Therefore, they are not adequate for understanding individual clouds, especially their three-dimensional shape and physical properties.

In this study, we try to extract and classify 3D clouds from cloud-resolving simulation data according to their 3D shape and physical properties. The details of the proposed cloud extraction and the classification method and its application results are reported.

2 Data set

The atmospheric simulation data used in this study is produced by the NICAM. The NICAM was first developed for the Earth Simulator and currently is also carried out on the K computer. The grid model uses an icosahedral grid structure and the horizontal resolution of the computational mesh is approximately 3.5 km. This model employs fully compressible non-hydrostatic equations to obtain statistically equilibrium states and guarantees the conservation of mass and energy. Equations are discretized by finite volume method. One characteristic feature of this model is that it explicitly calculates deep convective circulations without using cumulus parameterizations. For details of the model, please see [2].

The output data includes water vapor (3D), quantities of cloud water (3D), cloud ice (3D), velocity field (3D), precipitation (2D), outgoing long radiation (OLR) (2D). A snapshot image of a simulation result is shown in Fig. 1. 2D distribution of clouds and precipitation are visualized by gray scale color and rainbow color, respectively. Several clouds and rainfall areas are reproduced on the ground as well as on the ocean. Analysis domain in section 3 (for method description and test) and section 4 (for application) are shown in squares with a red solid border.

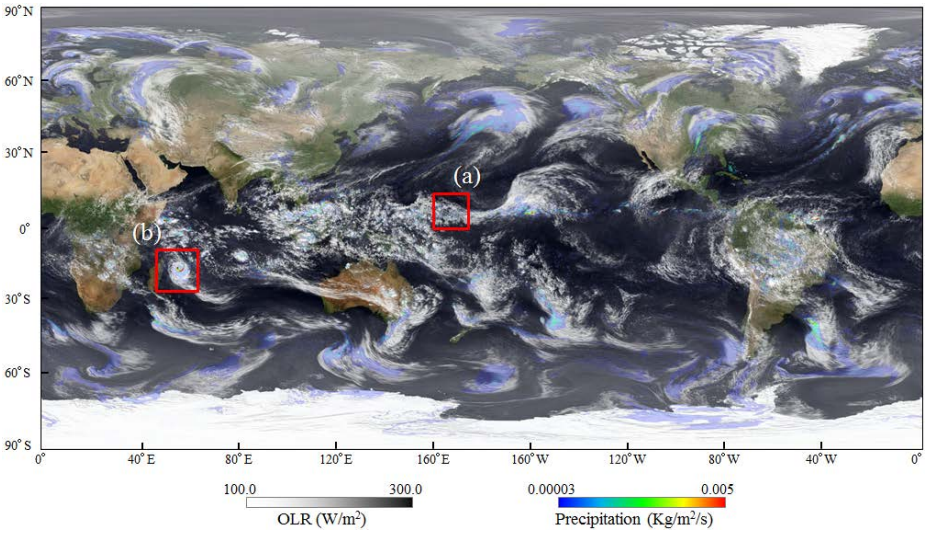

Fig. 1. A snapshot image of simulation results and analysis domain of (a) the Equatorial Pacific (Section 3) and (b) the Southern Indian Ocean (Section 4).

3 Method

3.1 Concept of proposed method

While real clouds have 3D configuration, previous work on cloud classification has not considered vertical distribution, as mentioned in Section 1. The general cloud forms have been standardized and published in the International Cloud Atlas by World Meteorological Organization (WMO) [12] as shown in a basic reference for schematic clouds types in Fig. 2 (a). In this reference, clouds are roughly classified into ten types such as cirrus, stratus and cumulus based on their altitude and physical properties.

Simulated clouds by numerical model do not correspond to all cloud forms because some cloud forms cannot be reproduced by the current physical scheme and spatial resolution. Hence, this study proposes a new simple and basic 3-dimensionall (3D) classification method for simulated clouds based on their altitude and upward flow. The proposed method classifies 3D clouds into the following six types, as shown in Fig. 2 (b): (1) cumulonimbus, (2) cumulus, (3) low-middle clouds, (4) low clouds, (5) middle clouds and (6) high clouds. Compared to the ten type classification by WMO, a couple of cloud forms are lamped together to one group. For example, altostratus and altocumulus are grouped as middle clouds.

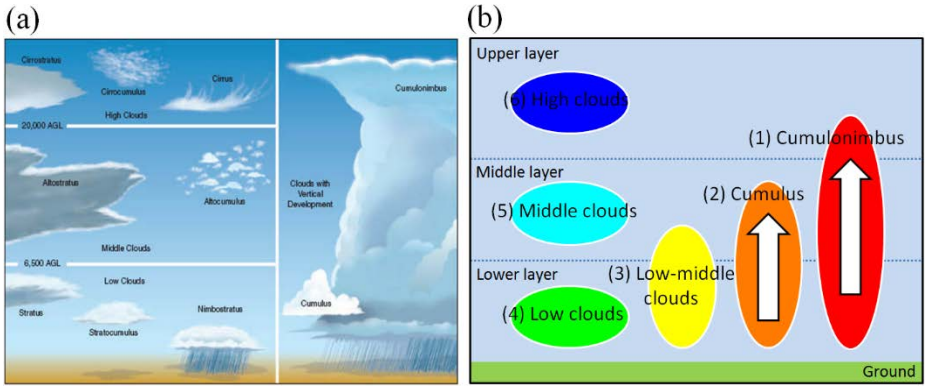

Fig. 2. Classification of clouds. (a) Ten types cloud classification by WMO [12] and (b) a conceptual image of six types cloud classification (proposed method).

3.2 Extraction of Clouds

A cloud is a visible mass of liquid or solid droplets made up of tiny water droplets or ice crystals, usually a mixture of both. In this study, clouds are detected from 3D simulation data on each grid point, where $qc + qi \geq qth$. Here, *qc*, *qi* and *qth* are quantity of cloud water, quantity of cloud ice and the threshold value for cloud detection, respectively. Individual cloud mass is defined by the spatially contiguous grid points that meet the conditions of cloud water and cloud ice. The algorithm is shown below.

```
## Algorithm 1: Extraction of clouds
SET ic to 1
```

```
SET cloud[i][j][k] to 0
FOR all grid point[i][j][k]
  IF cloud[i][j][k]=0 THEN
    IF qc[i][j][k]+qi[i][j][k]>qth THEN
      CALL search_cloud(i, j, k, ic);
      cloud_type[ic] = 3456
      ic = ic + 1
    ELSE
      cloud[i][j][k] = -999
    ENDIF
  ENDIF
END FOR

search_cloud(i, j, k, ic){
  IF cloud[i][j][k]=0 THEN
    IF qc[i][j][k]+qi[i][j][k]>qth THEN
      cloud[i][j][k] = ic
      search_cloud(i+1, j  , k  , ic)
      search_cloud(i-1, j  , k  , ic)
      search_cloud(i  , j+1, k  , ic)
      search_cloud(i  , j-1, k  , ic)
      search_cloud(i  , j  , k+1, ic)
      search_cloud(i  , j  , k-1, ic)
    ELSE
      cloud[i][j][k] = -999
    ENDIF
  ENDIF
}
```

Above algorithm explores unexplored grid points to the contiguous six directions (two direcions of longitude, latitude and altitude) from seed point in order to indentify identical cloud. This algorithm is a recursive algorithm that repeatedly uses the subroutine `search_cloud()` for exploring neighboring grid points. If the currently explored grid point fulfills the condition of cloud detection, the grid point is grouped with the identical clouds and stored as the candidate for the next seed point. Repeating this recursive process, the algorithm can identify an individual cloud. `cloud[i][j][k]` indicates an existence of a cloud on each grid point (1, 2, 3…: cloud, 0: candidate of cloud, -999: not cloud). An integer value of 1 or more indicates the identification number (`ic`) for individual cloud mass.

Figure 3 (a) depicts an extraction result of 3D clouds by using the proposed method (here, *qth* = 0.0001 kg/kg). However, Fig. 3 (b) depicts 2D clouds visualized by OLR (same figure with Fig. 1). While both results roughly correspond with each other, the shapes of the cumulonimbus are slightly different. Cumulonimbus with vertical flow is known to not be able to move upward beyond the boundary of the troposphere, and it

spreads widely in a horizontal direction [13]. This spread cloud at the top of cumulonimbus is called an anvil or incus (red dashed line in Fig. 3(a)). While Fig. 3 (b) represents the horizontal distribution of an anvil, Fig. 3 (a) clearly visualizes 3D configurations of cumulonimbus with an anvil.

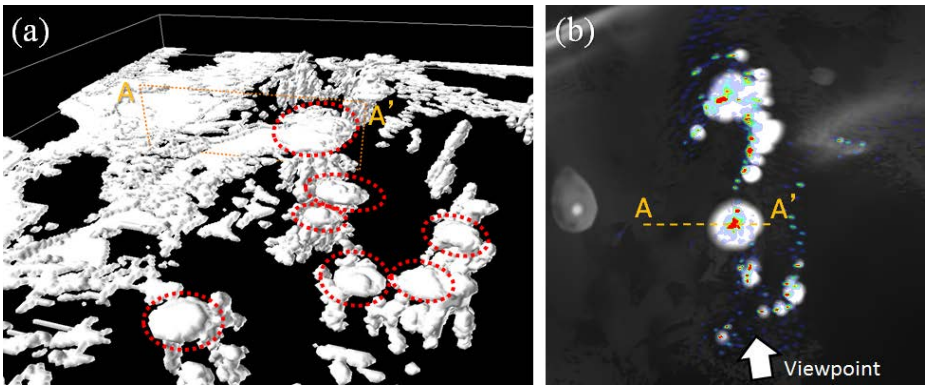

Fig. 3. Visualization results of clouds in (a) 3D (proposed method) and (b) 2D (same as Fig. 1).

In some cases, the abovementioned algorithm has a problem to be solved. There is a case where vertically developed clouds such as cumulonimbus and cumulus partially connect horizontally distributed clouds such as lower clouds, as shown in Fig. 4 (a). Separating these essentially different clouds using an additional physical property is necessary. Figure 4 (b) depicts upward flow (vertical component of velocity field) in clouds represented in Fig. 3 (yellow dashed line). While the magnitude of upward flow of the cumulonimbus is greater than 0.2 m/s (anvil cloud is 0.0-0.2 m/s), the same value of the lower cloud is 0.0-0.02 m/s. Therefore, they can be separated using the threshold value of upward flow.

Our proposed cloud extraction method is organized in two steps, cumulonimbus/cumulus extraction (Algorithm 2) and other clouds extraction (Algorithm 1). Algorithm 2 to extract cumulonimbus and cumulus is listed below.

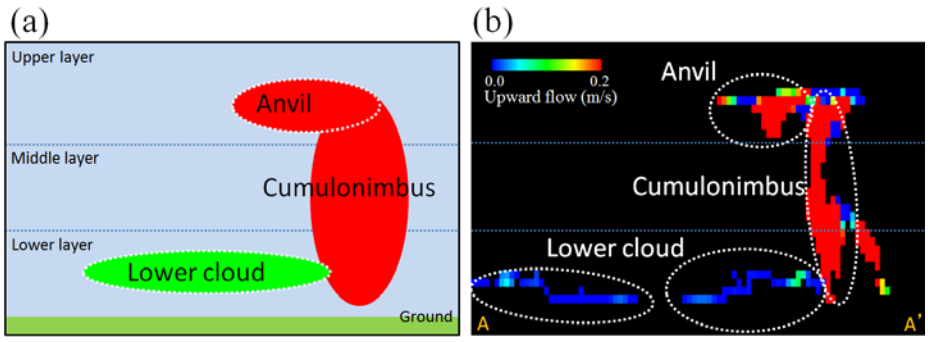

Fig. 4. Handling of connected clouds. Vertical image of (a) cloud form and (b) upward flow.

```
## Algorithm 2: Extraction of cumulus and cumulonimbus
FOR all grid point[i][j][k]
  IF cloud[i][j][k]=0 & alt[k]<7000.0 THEN
    IF qc[i][j][k]+qi[i][j][k]>qth & w[i][j][k]>wth THEN
      CALL search_cloud12(i, j, k, nc);
    ELSE
      cloud[i][j][k] = -999
    ENDIF
  ENDIF
  cloud_type[nc] = 12
  ic = ic + 1
END FOR
IF cloud[i][j][k] != 12 THEN
  SET cloud[i][j][k] to 0
ENDIF

search_cloud12(i, j, k, ic){
  IF cloud[i][j][k]=0 THEN
    IF alt[k]<7000.0 & qc[i][j][k]+qi[i][j][k]>qth
                                          &w[i][j][k]>wth
    || alt[k]>=7000.0 & qc[i][j][k]+qi[i][j][k]>qth THEN
      cloud[i][j][k] = ic
      search_cloud12(i+1, j  , k  , ic)
      search_cloud12(i-1, j  , k  , ic)
      search_cloud12(i  , j+1, k  , ic)
      search_cloud12(i  , j-1, k  , ic)
      search_cloud12(i  , j  , k+1, ic)
      search_cloud12(i  , j  , k-1, ic)
    ELSE
      cloud[i][j][k] = -999
    ENDIF
  ENDIF
}
```

The above listed algorithm is carried out before line 3 in Algorithm 1. The difference between Algorithm 2 and Algorithm 1 is whether the condition of cloud extraction includes threshold value of upward flow (here, *wth* = 0.2 m/s) or not. Furthermore, in order to extract an anvil cloud, when the altitude of an explored grid point is higher than 7000.0, the threshold value *wth* is not included in the condition of cumulonimbus/cumulus detection. The value of `cloud_type[ic]`, the unique ID number of the `ic`-th cloud, is 12 for cumulonimbus/cumulus and 3456 for other clouds. The separation result of both cloud forms is represented in Fig. 5. Pale red and pale blue clouds indicate cumulonimbus/cumulus and other clouds, respectively. This separation is a preparation for the six type cloud classification as mentioned in 3.3.

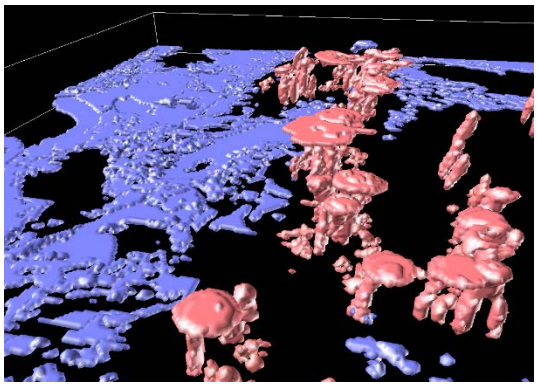

Fig. 5. Separation of cumulonimbus/cumulus and other clouds.

3.3 Classification of Clouds

Detected cumulonimbus and cumulus (`cloud_type[ic]=12`) are classified into the following two types based on their altitude: (1) lower to upper layer and (2) lower layer to middle layer, respectively. In the same way, other types of detected clouds (`cloud_type[ic]=3456`) are classified into the following four types: (3) lower to middle layer, (4) lower layer, (5) middle layer and (6) upper layer. The algorithm is shown below.

```
## Algorithm 3: Classification of clouds
FOR EACH cloud[ic]
  IF cloud_type[ic] = 12 THEN
    IF 3000.0<alt_min[ic] & 7000.0<=alt_max[ic] THEN
      cloud_type[ic] = 1
    IF alt_min[ic]<3000.0 THEN
      cloud_type[ic] = 2
    ENDIF
  ELSE IF cloud_type = 3456 THEN
    IF 7000.0<=alt_min[ic]
      cloud_type[ic] = 6
    ELSE IF 3000.0<=alt_min[ic] & alt_max[ic]<7000.0 THEN
      cloud_type[ic] = 5
    IF alt_max[ic]<3000.0 THEN
      cloud_type[ic] = 4
    ELSE IF alt_min[ic]<3000.0 & alt_max[ic]<7000.0 THEN
      cloud_type[ic] = 3
    ENDIF
  ENDIF
END FOR
```

The classification results are represented in Fig. 6. Figure 6 (a) is a result of using both Algorithm 1 and Algorithm 2, and Fig. 6 (b) is a result of using only Algorithm 1. In both results, extracted clouds are colored by red (cumulonimbus and anvil), orange (cumulus), yellow (low-middle clouds), green (low clouds), cyan (middle clouds) and blue (high clouds), as shown in Fig. 2(b). Compared to Fig. 6 (b), cumulonimbus with anvil and cumulus are correctly separated from other clouds in Fig. 6 (a).

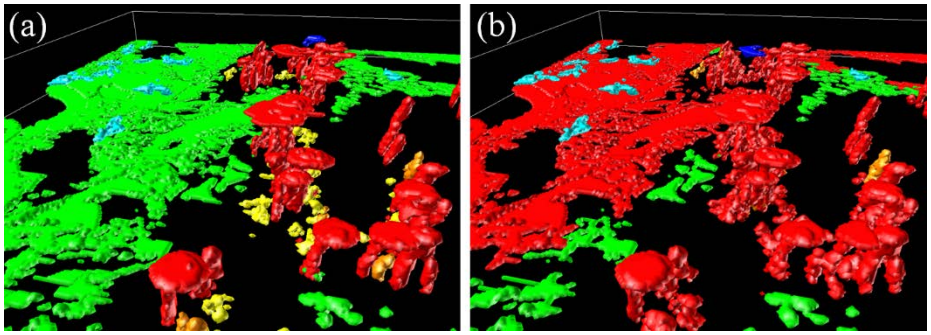

Fig. 6. Classification results (a) using cumulonimbus/cumulus separation (Algorithm 1 and Algorithm 2) and (b) simple cloud extraction (only Algorithm 1).

4 Results

The proposed method is applied to visualize tropical cyclones on the Indian Ocean in December 2011 simulated by NICAM (3.5km mesh). Tropical cyclones are known to have swirling clouds that are vertically developed [14, 15]. Its 2D (horizontal or vertical) structure has been studied; however, its 3D structure is not understood especially from the perspective of an individual cloud form.

Figure 7 displays visualization results of a tropical cyclone using the proposed six type cloud classification during December 1–8, 2011. The color of each cloud is shown in Fig. 2 (b). In the initial stage of the tropical cyclone, cumulonimbus and cumulus are developed, and low clouds and low-middle clouds gather around them because of decreasing pressure in the lower atmosphere (Fig. 7 (a)-(d)). In the developing stage, such clouds are swirled around the cumulonimbus, and the eye and eye wall (which is a wall of cumulonimbus around the eye) are formed (Fig. 7 (e)-(f)). This vortex structure, including swirled clouds, the eye and the eye wall, is called a tropical cyclone. In the fully developed stage, the size and the intensity of the tropical cyclone are developed to the maximum (Fig. 7 (g)). In the dissipation stage, the altitude of the eye wall with upward flow becomes lower, and the size of the tropical cyclone also decreases (Fig. 7 (h)).

The relationship between cloud form and rainfall in a tropical cyclone in the fully developed stage (Fig. 7 (g)) are shown in Fig 8. Figure 8 (a) and (b) depicts 2D distribution of precipitation and cloud form, respectively. Cloud form is represented in the stack in the order of (1) cumulonimbus, (2) cumulus, (3) low-middle clouds, (4) low clouds, (5) middle clouds, and (6) high clouds. The heavy rain region in the vicinity of

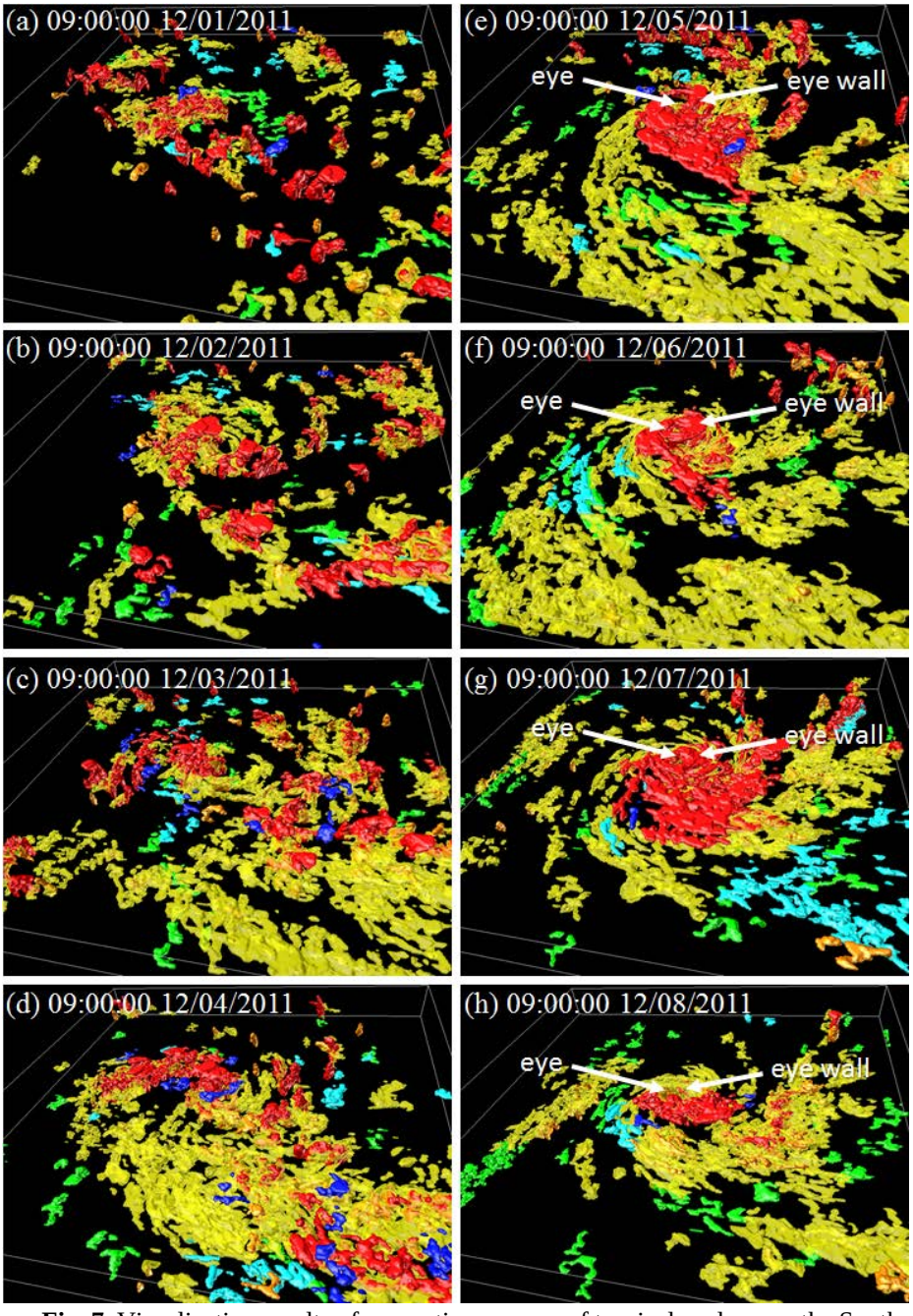

Fig. 7. Visualization results of generation process of tropical cyclone on the Southern Indian Ocean during December 1 to 8, 2011.

the eye of the tropical cyclone corresponds to cumulonimbus. Furthermore, we find that spiral-shape rain regions, called rain band inside red dashed line in Fig. 8 (a), correspond to the distribution of low-middle clouds.

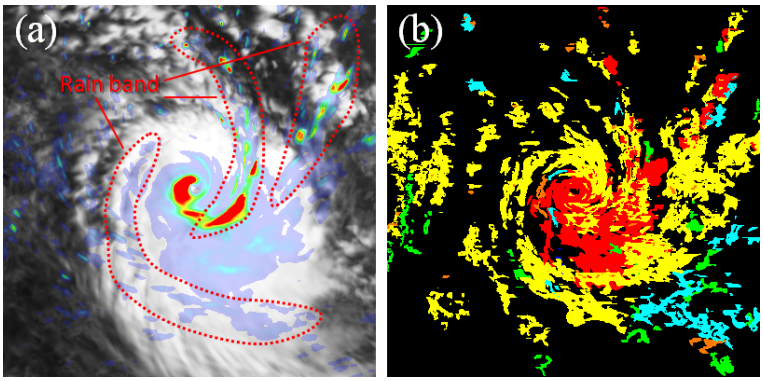

Fig. 8. Relation between (a) rainfall and (b) cloud form.

5 Summary and Discussion

In this study, we proposed a new extraction and classification method to intuitively understand simulated 3D clouds from cloud-resolving atmospheric simulation data. Extracted clouds are classified into six types using their altitude and vertical flow. As a result, we succeeded in visualizing the 3D structure of an atmospheric event such as a tropical cyclone from the perspective of individual 3D cloud forms. The proposed method is beneficial for understanding atmospheric phenomena. The proposed technique is expected to lead to the analysis of high-resolution atmospheric simulation data. However, it is noted that all of the threshold values, altitude, *qth* and *wth*, are given by user's trial and error, because typical physical values are not strictly defined to general cloud-forms. To determine physically correct threshold values for clouds, extraction and classification is required in future work.

Acknowledgement

We are grateful to Dr. Miyakawa (University of Tokyo), Dr. Nakano (JAMSTEC) and the NICAM team for their data production and model development. This work is supported by KAKENHI (26700010) Grant-in-Aid for Young Scientists (A).

References

1. Ohfuchi, W., Nakamura, H., Yoshioka, M. K., Enomoto, T., Takaya, K., Peng, X., Yamane, S., Nishimura, T., Kurihara, Y., Ninomiya, K.: 10-km Mesh meso-Scale Resolving Simulations of the Global Atmosphere on the Earth Simulator –Preliminary Outcomes of AFES (AGCM for the Earth Simulator)-, Journal of the Earth Simulator, 1, 8-34 (2004)
2. Tomita, S., Sato, M.: A New Dynamical Framework of Nonhydrostatic Global Model using The Icosahedral Grid, Fluid Dynamics Research, 34, 6, 357-400 (2004)
3. Sato, M., Tomita, H., Yashiro, H., Miura, H., Kodama, C., Seiki, T., Noda, A. T., Yamada, Y., Goto, D., Sawada, M., Miyoshi, T., Niwa, Y., Hara, M., Ohno, T., Iga, S., Arakawa, T., Inoue, T., Kubokawa, H.: The Non-hydrostatic Icosahedral Atmospheric Model: Description and Development, Progress in Earth and Planetary Science, 1, 18, 1-32 (2014)
4. Miura, H., Satoh, M., Nasuno, T., Noda, A. T., Oouchi, K.: A Madden-Julien Oscillation Event Realistically Simulated by a Global Cloud-Resolving Model, Science, 318, 1763-1765 (2007)
5. Nakano, M., Sawada, M., Nasuno, T., Satoh, M.: Intraseasonal Variability and Tropical Cyclonenesis in the Western North Pacific Simulated by a Global Nonhydrostatic Atmospheric Model, Geophysical Research Letter, 42, 565-571 (2015)
6. Karlsson, K. -G.: Development of an operational cloud classification model, International Journal of Remote Sensing, 10, 687-693 (1989)
7. Macias-Macias, C., Garcia-Orellana, C. J., Gonzales-Velasco, H., Gallardo-Caballero, R.: ICA and GA Feature Extraction and Selection for Cloud Classification, Lecture Note in Computer Science, 3686, 488-496 (2005)
8. Zibert, M. I., Derrien, M., Le Gleau, H.: Automatic Cloud Classification by Supervised Lerning on SEVIRI Data using Support Vector Machines Method, The 2005 EUMETSAT Meteorological Sattelite Conference, 188-192 (2006)
9. Kazantzidis, R., Tzoumanikas, P., Bais, A. F., Fotopoulos, S., EconomouU, G.: Equipment and Methodologies for Cloud Detection and Classification: A Review, Solar Energy, 95, 392-430 (2012)
10. Heinle, A., Macke, A., Srivastav, A.: Automatic cloud classification of whole sky images, Atmospheric Measurement Techniques, 3, 557-567 (2010)
11. Liu, S., Zhang, Z., Mei, X.: Ground-based cloud classification using weighted local binary patterns, Journal of Applied Remote Sensing, 9, 1, 095062 (2015)
12. The Ten Cloud Types, http://www.weathergamut.com/2011/10/14/cloud-nine/
13. Sinkevich, A. A., Krauss, T. W., Stepanenko, V. D., Dovgalyuk, Y. A., Veremey, N. E., Krov, A. B., Pivovarova, L. V.: Study of dynamics of the cumulonimbus anvil of large vertical extent, Russian Meteorology and Hydrology, 34, 12, 775-783 (2010)
14. Houze, R. A.: Clouds in Tropical Cyclones, Monthly Weather Review, 138, 293-344 (2010)
15. Oouchi, K., Fudeyasu, H. (Eds.): Cyclones: Formation, Triggers and Control, NOVA Publishers, New York (2012)